Ultrafast Optical Pump-Probe Studies of the Cytochrome b_6f Complex in Solution and Crystalline States

Naranbaatar Dashdorj[1,3], Eiki Yamashita[2,4], John Schaibley[1], William A. Cramer[2], and Sergei Savikhin[1,]*

[1]Department of Physics and [2]Department of Biological Sciences, Purdue University, West Lafayette, IN 47907

[3]Present address: Laboratory of Chemical Physics, NIDDK, National Institutes of Health, Bethesda, MD 20892

[4]Present address: Institute for Protein Research, Osaka University, Osaka, Japan

The running head: Ultrafast study of b_6f crystals

* Corresponding author, tel: (765) 294-3015, email: sergei@physics.purdue.edu

ABSTRACT. The cytochrome b_6f complex of oxygenic photosynthesis contains a single chlorophyll *a* (Chl *a*) molecule whose function is presently unknown. The singlet excited state of the Chl *a* molecule is quenched by the surrounding protein matrix, and thus the Chl *a* molecule in the b_6f complex may serve as an exceptionally sensitive probe of the protein structure. For the first time, singlet excited state dynamics were measured in well-diffracting crystals using femtosecond time-resolved optical pump-probe methodology. Lifetimes of the Chl *a* molecule in crystals of the cytochrome b_6f complex having different space groups were 3-6 times longer than those determined in detergent solution of the b_6f. The observed differences in excited state dynamics may arise from small (1 – 1.5 Å) changes in the local protein structure caused by crystal packing. The Chl *a* excited state lifetimes measured in the dissolved cytochrome b_6f complexes from several different species are essentially the same, in spite of differences in the local amino acid sequences around the Chl *a*. This supports an earlier hypothesis that the short excited state lifetime of Chl *a* is critical for the function of the b_6f complex.

KEYWORDS: Chlorophyll *a*; cytochrome b_6f complex; membrane proteins, protein crystals, packing; ultrafast spectroscopy

INTRODUCTION

To date, approximately 45,000 independent structures of soluble, and approximately 150 of integral membrane proteins have been solved, most of the latter using X-ray crystallography. Crystallographic structure determination requires that proteins self-assemble into a densely packed crystal grid. Crystal contacts involve a significant portion of the solvent-accessible surface of a protein and may induce structural changes. This possibility prompts a question about whether the protein structure is perturbed by crystal contacts. One way to address this question is to compare X-ray structures of proteins with the ensemble of soluble conformers of the same proteins determined by NMR.[1,2] However, the number of membrane protein structures solved by both methods is very limited. Moreover, due to the broadening of the NMR line-widths with increased molecular weight, there is an upper limit of protein molecular weight (~50 kDa) for which an NMR structure can be determined. Another approach is to analyze differences between the X-ray structures of the same protein in different crystal packing environments, which has been done for several specific proteins, such as eglins, basic pancreatic trypsin inhibitors, MurD ligases, and signal recognition particles.[3-6] However, the latter approach does not provide direct information on deviations of the protein crystal structure from that in its natural setting.

In the present study, sensitive ultrafast spectroscopy is used to probe small differences between the solution and crystal structure of a large hetero-oligomeric integral membrane protein complex, the cytochrome b_6f of oxygenic photosynthesis. This complex provides the opportunity to probe such differences in structure because of the presence of only one pigment (chlorophyll *a*) molecule in this complex, and the dependence of the lifetime of this chlorophyll on local protein structure.

The b_6f complex (Fig. 1A) consists of four large (cytochrome *f*, cytochrome b_6, the Rieske iron-sulfur protein, subunit IV), and four small subunits (PetG, PetL, PetM, PetN) arranged in a functionally active dimeric form with a total molecular weight of ~217 kDa.[7,8] In oxygenic photosynthesis, the cytochrome b_6f complex mediates electron transfer between the reaction centers of photosystems I and II and mediates coupled proton translocation across the membrane.

Three-dimensional crystal structures of the cytochrome b_6f complex from the thermophilic cyanobacterium *Mastigocladus laminosus* have been obtained at a resolution of 3.0 Å.[9,10] A highly homologous crystal structure of the complex from the unicellular green alga *Chlamydomonas reinhardtii* in the presence of the quinone-analogue inhibitor tridecyl-stigmatellin has also been determined at a resolution of 3.1 Å.[11] The crystal structures of the b_6f complex reveal two noncovalently bound pigments, a Chl *a* and a β-carotene, with unitary stoichiometry per monomer (**Fig. 1A**). This makes the b_6f complex the only known pigment-protein complex that contains a single pigment (Chl *a*) molecule, making it a unique system, in which intraprotein pigment-protein interactions can be studied without interference from other pigment molecules, as first recognized by Peterman et al.[12] The role of the Chl *a* in the b_6f complex is still a mystery. The function of this complex does not require light harvesting, and the Chl *a* is not part of the electron transfer chain, which are the common functions of chlorophyll molecules in photosynthetic reaction center complexes. Furthermore, the introduction of a chlorophyll molecule into the protein may jeopardize the stability of the complex because of photo-damage resulting from the generation of singlet oxygen. The possible role of the Chl *a* molecule in the b_6f complex has been discussed extensively in the literature.[10,11,13-16]

The Chl *a* molecule in the b_6f complex has an unusually short singlet excited state lifetime of ~200 ps, which is ~25 times shorter than that for Chl *a* in solution.[12,14] It has been inferred that

the singlet excited state of the Chl *a* molecule is quenched due to the excitation-induced electron transfer interaction with a nearby aromatic amino acid residue, and it was proposed that this process has an important functional role in protecting the complex against harmful singlet oxygen.[14] The electron transfer rate depends strongly on the distance between the amino acid residue and the Chl *a* porphyrin ring system. The unitary pigment stoichiometry of the Chl *a* molecule in the b_6f complex and its singlet excited state lifetime, which is highly dependent on the surrounding protein matrix, makes this Chl *a* molecule an unprecedented structural probe of the hetero-oligomeric protein structure, which is readily accessible to ultrafast optical spectroscopy.

In the present study, we have measured the singlet excited state lifetime and the ground state recovery of the Chl *a* molecule of the cytochrome b_6f complex in crystals with two different packing arrangements, as well as in re-dissolved diffraction quality crystals, using femtosecond time-resolved optical techniques. Presently, there are no reports on the application of femtosecond time-resolved optical pump-probe measurements to protein crystals that yield meaningful x-ray diffraction data. Transient fluorescence and steady-state optical studies have been performed on single crystals (see, for example, measurements on crystals of photoactive yellow protein,[17] bacteriorhodopsin,[18] LHC-II[19] and FMN binding protein[20]). In conceptually different time-resolved X-ray experiments, dynamics of proteins were probed with ~100 ps time resolution,[21-23] but no comparison with proteins in a native environment could be made. The femtosecond pump-probe experiments in the present study revealed a large difference between the solution and crystalline states in the picosecond singlet excited state dynamics of the Chl *a* molecule, which are most readily interpreted in terms of small but significant differences in the local protein structure.

EXPERIMENTAL METHODS

Protein purification and crystallization

Purification and crystallization of the cytochrome b_6f complex from the thermophilic cyanobacterium *Mastigocladus laminosus* have previously been described in detail.[24,25] The crystals of two different symmetries ($P6_122$ and $P2_12_12$, Fig. 1B,C) used in the spectroscopic experiments had a 1.0:1 stoichiometry of Chl *a* relative to cytochrome *f*, and contained complexes in a functionally active form exhibiting an electron transfer rate of ~ 200 electrons (cyt *f*)$^{-1}$s^{-1} for electron transfer from decyl-plastoquinol to plastocyanin-ferricyanide.[25] The unit stoichiometry of Chl *a* relative to cytochrome *f* was critical for unambiguous interpretation of the experimental results, as a larger value of the stoichiometry indicates the presence of adventitiously bound chlorophyll with much longer excited state lifetimes. To ensure the highest sample purity, the sample with solvated complexes was prepared by diluting approximately sixty X-ray diffraction quality single crystals of the cytochrome b_6f complex from *M. laminosus* in a buffer containing 30 mM Tris•HCl (pH 7.5), 50 mM NaCl, and 0.05% undecyl-β-D-maltoside.[14] For low temperature measurements, glycerol was added to the sample to constitute 65% by volume to eliminate sample cracking upon freezing and produce a good optical quality glass. Addition of glycerol did not affect spectroscopic and kinetic properties of the Chl *a* within the complex.

Spectroscopic measurements

Steady state absorption spectra of dissolved crystal samples were measured at room temperature (RT) using a Lambda 3B spectrometer (Wellesley, MA). An XSpectra single crystal

microspectrometer (4DX Systems, Uppsala, Sweden) was used to measure steady state absorption spectra of single crystals.

For time-resolved experiments, excitation pulses (630 nm, ~100 fs fwhm) were generated by an optical parametric amplifier pumped by an amplified femtosecond Ti:Sapphire laser system described earlier.[26] Transient sample absorption was probed with a broad-band femtosecond light continuum generated in a sapphire plate; the cross-correlation between the pump and probe pulses was typically 100 – 200 fs fwhm. Continuum probe pulses were split into signal and reference beams, dispersed in an Oriel MS257 imaging monochromator (Stratford, CT) operated at ~ 3 nm bandpass and directed onto separate Hamamatsu S3071 Si pin photodiodes. The probe, reference, and pump pulse energies were measured in Stanford Research Systems SR250 boxcar integrators (Sunnyvale, CA), digitized, and computer-processed. The noise level was near the shot noise-limitation; the root mean square noise in ΔA was ~3×10^{-5} for a 1 s accumulation time. For room temperature experiments, dissolved crystal samples were housed in a cell with a 1 mm path length and exhibited ~ 0.3 absorbance at 670 nm. Crystals with size ~100 x 80 x 30 μm were mounted in a custom designed cell. The absorbance of crystals at an excitation wavelength of 630 nm was ~0.2. Small amounts of the solution from the crystallization well were added to avoid drying of the crystals.

For low temperature studies, 5 μl of b_6f crystals dissolved in buffer containing 65% glycerol were placed between two optical flats separated and sealed by 0.7 mm thick rubber spacer and attached to the cold finger of a closed cycle cryostat (Air Products DE-202/HC-2/APD-E, Allentown, PA). The temperature in the sample was controlled to within 5 K and was varied between 25 K and RT.

RESULTS

Crystal packing

The crystal packing of the two single b_6f crystals with $P6_122$ (hexagonal) and $P2_12_12$ (orthorhombic) space groups is shown in **Fig. 1B, C**. For the hexagonal crystal (**Fig. 1B**), an asymmetric unit contains a monomer of the b_6f complex and a high solvent content (78%). The crystallographic two-fold axis coincides with the two-fold axis of the dimer. Crystal packing involves two types of contacts, both involving cytochrome *f*: (i) cytochrome *f* – cytochrome *f*; (ii) cytochrome *f* against the *n*- (stromal) side of the complex including subunit IV and cytochrome b_6. The orthorhombic crystal also contains one dimer per asymmetric unit, with the molecular two-fold axis coinciding with a crystallographic axis (**Fig. 1C**). Crystal contacts consist of two kinds that resemble those in the crystal with $P6_122$ hexagonal packing, although the relative tilt angles are different.

According to the crystal structures[9-11] of the b_6f complex, the monomeric Chl *a* ring is inserted between F and G helices of subunit IV, with the phytyl tail wrapped around part of the F helix (**Fig. 1D**). The loop regions of the F and G helices are directly involved in the crystal packing contacts as shown in **Fig. 1D**, which may cause long-range distortion and affect the protein structure around the Chl *a*, as well as its optical properties.

Absorbance spectra of the cytochrome b_6f complex in solution and in crystals

The absorbance spectra of diffraction quality crystals in the hexagonal $P6_122$ space group (b_6f-hexa), the orthorhombic $P2_12_12$ space group (b_6f-ortho), and dissolved crystals of the cytochrome b_6f complex (b_6f-dissolved) in the spectral region 600 – 735 nm are shown in **Fig. 2**. The main band in the absorbance spectra is due to the Q_y band of the Chl *a* molecule, whereas the peak at ~625 nm arises primarily from the vibrational bands of the Chl *a* molecule. The Chl *a*

Q_y bands in the b_6f-dissolved and b_6f-hexa are the same within experimental resolution. The absorbance bands have maxima at ~671.5 nm and a fwhm of ~17 nm, whereas in the b_6f-ortho crystal, the Q_y band of Chl *a* is centered at the same wavelength, but has a somewhat larger fwhm of ~20 nm. The mutual orientation of the probe light polarization and crystallographic axis could not be determined in these measurements. Measurements on a series of different crystals with varying probe light polarization resulted in <10% variations in the bandwidth of the Chl *a* Q_y band, but no variations in the Q_y maximum position were detected.

The singlet excited state kinetics of the monomeric Chl a in the cytochrome b_6f complex

The Chl *a* of the b_6f complex in all samples was excited at 630 nm and the dynamics of the absorbance changes, ΔA, were recorded at multiple probe wavelengths covering the entire Q_y absorption band of the Chl *a*. The picosecond excited state decay is reflected in the kinetics of the absorbance difference probed at 680 nm for all three samples (**Fig. 3**).

As discussed previously,[14] the kinetics of Chl *a* excited state in b_6f -dissolved can be described by a major component of 200 ± 20 ps (1/e decay time) in the decay of the absorbance change of the Q_y band, and were found to vary slightly depending on sample preparation. The decay times measured with the crystals are, however, substantially longer. The absorbance difference profiles obtained for the b_6f-hexagonal crystal could be fit with a major decay component of 1100±150 ps. A two-exponential fit to the experimental data for the b_6f-ortho crystal yielded singlet state decay times of 860±100 ps (amplitude, 66%) and 110±15 ps (34%). The global analysis of kinetic profiles probed between 660 nm and 700 nm (5 nm sampling interval) resulted in decay-associated spectra (DAS), which showed that these major decay components arise from the Chl *a* excited/ground state dynamics (**Fig. 4**), as their amplitude dependence on the probe wavelength

mimicked the absorbance spectrum of the Chl *a* (Fig. 2). Several weaker components found in the DAS may arise from a small heterogeneous pool of nonspecifically bound Chl *a* and from vibrational relaxation of the Chl *a* excited state.[14]

Cooling the b_6f-dissolved sample from RT down to 25 K did not affect the dynamics of Chl *a*, and ΔA profiles could be described by the same major decay time of 200±20 ps. The kinetics became slightly longer at 200 K and the fit to the data yielded a major lifetime component of 240±20 ps. This lifetime lengthened to 270±20 ps upon cooling the sample below 180 K, did not change upon further cooling to 25 K, which is consistent with the temperature dependence of physical properties of the solvent (glycerol/water) used to dissolve b_6f complexes for low temperature studies. The viscosity of this mixture significantly increases at temperatures below its melting point (T_m ~ 235 K), and it is known to form a glass-like substance below its glass transition temperature at T_g ~ 180 K.[27] The kinetic profile measured at 25 K is shown in Fig. 3. It can be noted that the effect of temperature on the Chl *a* lifetime in the b_6f complex is significantly weaker than the effect of crystallization.

Figure 5 shows the time-resolved transient absorption difference profiles probed at 680 nm following excitation at 630 nm for the same preparation of cytochrome b_6f complex diluted in different solvents. Glycerol, 70 % by volume, was added to the sample dissolved in the original buffer to alter both the refractive index and dielectric constant of the medium surrounding the b_6f complex. In the other sample, 5% PEG was added to mimic the crystal growth medium. In both of these samples, the kinetics of the Chl *a* excited state were the same as in the sample dissolved in standard buffer.

DISCUSSION

It was shown that the Chl *a* molecule in the cytochrome b_6f complex in solution has an unusually short singlet excited state lifetime of ~200 ps that is characteristic of both the enzymatically active dimeric b_6f complexes[14] and the functionally inactive monomeric cytochrome b_6f complexes.[12,14] The 200 ps excited state lifetime contrasts with the 5 – 6 ns lifetime reported for monomeric Chl *a* in solution,[28] which is ~25-fold longer. After a thorough examination of possible causes of the observed rapid quenching of the Chl *a* singlet excited state, it was inferred that the excitation-induced electron transfer between the Chl *a* and nearby aromatic amino acid residue(s) is the most likely explanation for the observed effect.[14] Because intra-protein electron transfer rates depend strongly on the distance between the donor and acceptor molecules,[29,30] the Chl *a* molecule can serve as a structural probe of the surrounding protein structure.

The loop regions of the F and G helices that are directly involved in the crystal packing contacts (Fig. 3) may cause long-range distortion of the protein structure along these helices that results in a change of the distance between the Chl *a* and the quenching amino acid residue, which in turn alters the dynamics of the Chl *a* excited state. Alternatively, the deviations in the Chl *a* dynamics may stem from differences in overall medium characteristics like salt concentrations, pH values, solvent content, and protein concentrations of the crystals and dissolved b_6f samples. These factors may affect the refractive index and dielectric constant of the medium surrounding the protein and thereby the radiative lifetime of the Chl *a* excited state.[31-33] However, no variations were observed in the excited state lifetime of Chl *a* in the b_6f complexes dissolved in different solvents, in which refractive index and dielectric constant were varied by adding glycerol or using solvent analogous to the crystal growth media (Fig. 5). These data also exclude different water content of the two crystals as a possible cause of the observed variation

in Chl *a* lifetime. In addition, the local environment of the Chl *a* in single crystals and in the dissolved b_6f complex ought to be similar electrostatically, since no spectral shifts were observed in the steady-state absorption spectra (Fig. 2). Based on these data, we infer that the variations in lifetime of the Chl *a* excited state in different samples are caused by changes in local protein conformation that affect the rate of quenching mediated by electron transfer.

As inferred by Dashdorj *et al.*[14], the Chl *a* singlet excited state quenching mechanism occurs through excitation-induced electron transfer between the Chl *a* and surrounding amino acid residue(s). The effect of a change in the distance between the Chl electron donor and a nearby aromatic residue as electron acceptor can be estimated through the rate-distance relationships for long range electron transfer in proteins.[29,30] Using the Moser-Dutton semi-empirical relationship[29] for the dependence of the rate of electron transfer, k_{ET}, at room temperature on edge-to-edge distance between donor and acceptor, the Gibbs free energy change for the electron transfer ΔG^o, and the reorganization energy, the observed 5.5-fold increase in the Chl *a* excited state lifetime in the hexagonal crystal would be caused by an increase of ~ 1.2 Å in the distance between the Chl *a* and the quenching residue. On the other hand, the free energy change and reorganization energy, λ, may also be altered in a crystal. However, it is expected that the protein in the crystal is more rigid, which would imply a smaller λ and faster electron transfer rate, since $-\Delta G^o < \lambda$.[14] The application of the structure dependent rate-distance relationship for electron transfer in proteins[30] would not change the donor-acceptor distance change required to account for the increase of Chl excited state lifetime in crystals by more than 20 %, and it would still be on the order of 1.0 – 1.5 Å for hexagonal crystal.

Quenching of the Chl *a* molecule could, in principle, be assisted by a large scale breathing motion of a protein that would dynamically change the distance to the quenching residue. Such a

protein motion may be affected by crystal packing. This scenario was proposed but not verified by Chosrowjan et al.[20] to explain the 20-fold longer lifetime of the excited state of flavin quenched by a similar electron transfer mechanism in the flavin binding protein in the crystal versus solution phase. If protein dynamics is essential for the Chl *a* quenching, one would expect a dramatic change in the Chl *a* lifetime in the dissolved b_6f complex at low temperatures. However, our experiments show only a slight change in that lifetime with a 10-fold change in temperature (Fig. 3), which indicates that protein motion plays only a minor role in the Chl *a* quenching process. The small changes in the Chl *a* lifetime at low temperatures appear to be associated with the change in the mobility of the solvent, which has been shown to be a dominant factor in determining the atomic fluctuations above 180 K.[34] The independence of the Chl *a* quenching dynamics in the 25 K - 180 K region also suggests that intrinsic protein motions are not involved in the quenching process.[34] Further analysis of these data requires precise knowledge of ΔG^o and λ., since electron transfer rates are temperature-dependent.[35]

As in the case of flavoproteins,[20,36] the location of the quenching residue in the cytochrome b_6f complex is still unknown. Trp and Tyr residues both have redox properties suitable for quenching, and most of them are conserved between different species in the vicinity of the Chl *a*. It was earlier proposed[14] that the neighboring Tyr105 residue may serve as a Chl *a* quencher in the cytochrome b_6f complex. However, studies on a Tyr105Phe mutant have not confirmed that hypothesis (Yan *et al.*, in preparation). Studies on a Trp118Leu mutant also excluded its involvement. This narrows the list of the most probable quenchers to 4 residues, Trp79, Tyr80, Tyr82 and Trp142, which are all ≤12 Å from the Chl *a*. Unlike Tyr105 and Trp118 residues that are part of the cytochrome b_6 subunit, these four residues are all part of subunit IV, which binds the Chl *a* and is directly involved in crystal contact, and Trp142 is located in helix G (Fig. 1D).

In conclusion, these studies demonstrate that ultrafast optical pump-probe measurements can be performed on single x-ray quality crystals of proteins, and that the Chl *a* excited state lifetime in the b_6f complex is sensitive to the changes induced by crystal contacts that are remote from the immediate vicinity of the chromophore. On the other hand, the Chl *a* excited state lifetime in the b_6f complexes in solution is essentially the same for all studied sources—the cyanobacteria *M. Laminosus*, *Synechococcus* PCC 7002 and *Synechocystis* PCC 6803, and b_6f complex from spinach,[12,14] even though the amino acid sequence in the immediate vicinity of the chromophore is not fully conserved between these sources. Given the very precise dependence of electron transfer on distance, it is of interest that there are not larger variations in the short lifetime between the b_6f complexes from different organisms. Presumably, this is a result of conservation of the distances in the structure involved in the Chl quenching reaction.

It has been inferred previously that the quenching of the Chl *a* excited state is an important property that has a vital role in photo-protection of the b_6f complex that minimizes singlet oxygen formation.[14] Our data provide additional evidence that the short excited state lifetime of Chl *a* is a fundamental property of the cytochrome b_6f complex. It is inferred that the dramatic increase in the excited state lifetime of the Chl *a* in crystals of the b_6f complex arises from structure changes on the order of 1 – 1.5 Å.

Acknowledgments. This work was supported by a grant from the NSF, MCB-0516939 to SS and from the NIH, GM-38323, to WAC. The authors would like to thank H. Zhang, H. Kim, S. Kihara and T. Zakharova for contributions to the experiments. Some of the experiments were performed using Ames Laboratory equipment supported by the Division of Chemical Sciences, Office of Basic Energy Sciences, and U. S. Department of Energy. Ames Laboratory is operated by Iowa State University under Contract W-7405-Eng-82.

FIGURE CAPTIONS

Figure 1. (A) Structure of the dimeric cytochrome b_6f complex embedded in the thylakoid membrane. (B) The arrangement of the cytochrome b_6f complexes in hexagonal packing of crystal with $P6_122$ space group and (C) in orthorhombic packing crystal with $P2_12_12$ space group. (D) Inter-protein contact region (ellipse) in hexagonal packing crystal, which involves continuous loop regions of the F and G helices of subunit IV and cytochrome *f*. The color code for all panels: cytochrome b_6 (mauve); cytochrome *f* (red); subunit IV (light blue); ISP (yellow); PetG, PetL, PetM, and PetN (blue), Chl *a* (green), carotenoid (orange), hemes (white), Fe_2S_2 cluster (white and yellow).

Figure 2. Absorbance spectra of the b_6f-hexa, b_6f-ortho and b_6f-dissolved measured in the spectral interval of 600 – 735 nm at room temperature. The b_6f-hexa and b_6f-ortho absorbance spectra were normalized to the spectrum of dissolved b_6f (b_6f-dissolved).

Figure 3. Time-resolved transient absorbance difference profiles probed at 680 nm following excitation at 630 nm for b_6f-dissolved samples at RT and 25 K, and for b_6f-hexa, and b_6f-ortho samples at room temperature.

Figure 4. Decay-associated spectra obtained via global analysis of all absorbance difference profiles for the b_6f-dissolved, b_6f-hexa and b_6f-ortho samples at room temperature.

Figure 5. Time-resolved transient absorbance difference profiles probed at 680 nm at RT following excitation at 630 nm for (1) the original b_6f-dissolved sample, (2) the same sample in the buffer that contained 70 % of glycerol, and (3) the sample with 5 % PEG that that was present in the crystal growth medium.

REFERENCES

(1) Wagner, G.; Hyberts, S. G.; Havel, T. F. *Annu. Rev. Biophys. Biomol. Struct.* **1992**, *21*, 167-198.

(2) Garbuzynskiy, S. O.; Melnik, B. S.; Lobanov, M. Y.; Finkelstein, A. V.; Galzitskaya, O. V. *Proteins: Struct., Funct., Bioinf.* **2005**, *60*, 139-147.

(3) Kuglstatter, A.; Oubridge, C.; Nagai, K. *Nature Struct. Biol.* **2002**, *9*, 740-744.

(4) Heinz, D. W.; Priestle, J. P.; Rahuel, J.; Wilson, K. S.; Grütter, M. G. *J. Mol. Biol.* **1991**, *217*, 353-371.

(5) Kossiakoff, A. A.; Randal, M.; Guenot, J.; Eigenbrot, C. *Proteins: Struct., Funct., Genet.* **1992**, *14*, 65-74.

(6) Bertrand, J. A.; Fanchon, E.; Martin, L.; Chantalat, L.; Auger, G.; Blanot, D.; van Heijenoort, J.; Dideberg, O. *J. Mol. Biol.* **2000**, *301*, 1257-1266.

(7) Cramer, W. A.; Zhang, H.; Yan, J.; Kurisu, G.; Smith, J. L. *Annu. Rev. Biochem.* **2006**, *75*, 769-790.

(8) Whitelegge, J. P.; Zhang, H.; Taylor, R.; Cramer, W. A. *Mol. Cell. Proteomics* **2002**, *1*, 816-827.

(9) Yamashita, E.; Zhang, H.; Cramer, W. A. *J. Mol. Biol.* **2007**, *370*, 39-72.

(10) Kurisu, G.; Zhang, H.; Smith, J. L.; Cramer, W. A. *Science* **2003**, *302*, 1009-1014.

(11) Stroebel, D.; Choquet, Y.; Popot, J.-L.; Picot, D. *Nature* **2003**, *426*, 413-418.

(12) Peterman, E. J. G.; Wenk, S.-O.; Pullerits, T.; Pålsson, L.-O.; van Grondelle, R.; Dekker, J. P.; Rögner, M.; van Amerongen, H. *Biophys. J.* **1998**, *75*, 389-398.

(13) Kühlbrandt, W. *Nature* **2003**, *426*, 399-400.

(14) Dashdorj, N.; Zhang, H.; Kim, H.; Yan, J.; Cramer, W. A.; Savikhin, S. *Biophys. J.* **2005**, *88*, 4178-4187.

(15) Wenk, S.-O.; Schneider, D.; Boronowsky, U.; Jäger, C.; Klughammer, C.; de Weerd, F. L.; van Roon, H.; Vermaas, W. F. J.; Dekker, J. P.; Rögner, M. *FEBS J.* **2005**, *272*, 582-592.

(16) Pierre, Y.; Breyton, C.; Lemoine, Y.; Robert, B.; Vernotte, C.; Popot, J.-L. *J. Biol. Chem.* **1997**, *272*, 21901-21908.

(17) Yeremenko, S.; van Stokkum, I. H. M.; Moffat, K.; Hellingwerf, K. J. *Biophys. J.* **2006**, *90*, 4224-4235.

(18) Efremov, R.; Gordeliy, V. I.; Heberle, J.; Büldt, G. *Biophys. J.* **2006**, *91*, 1441-1451.

(19) Pascal, A. A.; Liu, Z.; Broess, K.; van Oort, B.; van Amerongen, H.; Wang, C.; Horton, P.; Robert, B.; Chang, W.; Ruban, A. *Nature* **2005**, *436*, 134-137.

(20) Chosrowjan, H.; Taniguchi, S.; Mataga, N.; Tanaka, F.; Todoroki, D.; Kitamura, M. *J. Phys. Chem. B* **2007**, *111*, 8695-8697.

(21) Schotte, F.; Lim, M.; Jackson, T. A.; Smirnov, A. V.; Soman, J.; Olson, S. O.; Phillips, G. N. J.; Wulff, M.; Anfinrud, P. A. *Science* **2003**, *300*, 1944-1947.

(22) Schotte, F.; Soman, J.; Olson, J. S.; Wulff, M.; Anfinrud, P. A. *J. Struct. Biol.* **2004**, *147*, 235-246.

(23) Anderson, S.; Srajer, V.; Pahl, R.; Rajagopal, S.; Schotte, F.; Anfinrud, P. A.; Wulff, M.; Moffat, K. *Structure (Camb)* **2004**, *12*, 1039-1045.

(24) Zhang, H.; Cramer, W. A. Purification and crystallization of the cytochrome b_6f complex in oxygenic photosynthesis. In *Photosynthesis research protocols*; Carpentier, R., Ed.; Humana Press Inc.: Totowa, NJ, 2004; pp 67-78.

(25) Zhang, H.; Kurisu, G.; Smith, J. L.; Cramer, W. A. *Proc. Natl. Acad. Sci. USA* **2003**, *100*, 5160-5163.

(26) Savikhin, S.; Xu, W.; Soukoulis, V.; Chitnis, P. R.; Struve, W. S. *Biophys. J.* **1999**, *76*, 3278-3288.

(27) Murthy, S. S. N. *Cryobiology* **1998**, *36*, 84-96.

(28) Seely, G. R.; Connolly, J. S. Fluorescence of photosynthetic pigments in vitro. In *Light emission by plants and bacteria*; Govindjee, J., Amesz, J., Fork, D. C., Eds.; Academic Press: New York, 1986; pp 99-133.

(29) Page, C. C.; Moser, C. C.; Chen, X.; Dutton, P. L. *Nature* **1999**, *402*, 47-52.

(30) Gray, H. B.; Winkler, J. R. *Quart. Rev. Biophysics* **2003**, *36*, 341-372.

(31) Suhling, K.; Siegel, J.; Phillips, D.; French, P. M. W.; Lévêque-Fort, S.; Webb, S. E. D.; Davis, D. M. *Biophys. J.* **2002**, *83*, 3589-3595.

(32) Toptygin, D.; Savtchenko, R. S.; Meadow, N. D.; Roseman, S.; Brand, L. *J. Phys. Chem. B* **2002**, *106*, 3724-3734.

(33) Lakowicz, J. R. *Principles of fluorescence spectroscopy*, 2nd ed.; Kluwer Academic and Plenum Publishers: New York, NY, 1999.

(34) Vitkup, D.; Ringe, D.; Petsko, G. A.; Karplus, M. *Nature Struct. Biol.* **2000**, *7*, 34-38.

(35) Moser, C. C.; Dutton, P. L. *Biochim. Biophys. Acta* **1992**, *1101*, 171-176.

(36) Zhong, D.; Zewail, A. H. *Proc. Natl. Acad. Sci. USA* **2001**, *98*, 11867-11872.

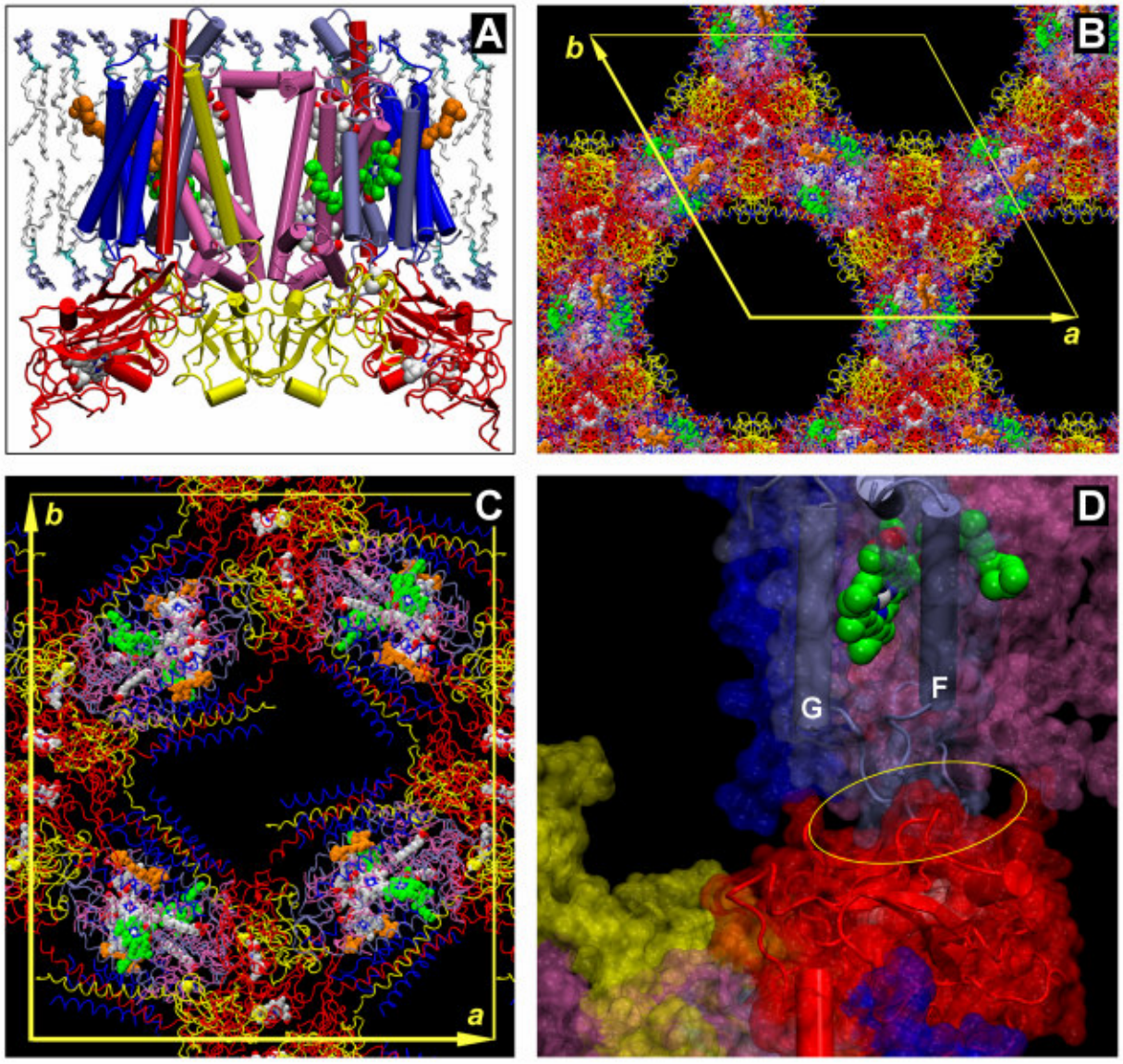

Figure 1

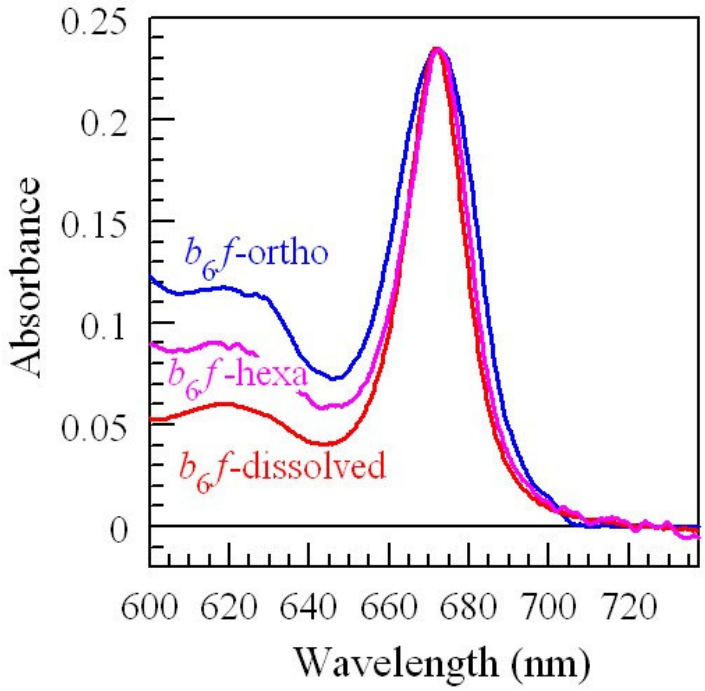
0.25
0.2
0.15
0.1
0.05
0
Absorbance
b_6f-ortho
b_6f-hexa
b_6f-dissolved
600 620 640 660 680 700 720
Wavelength (nm)

Figure 2

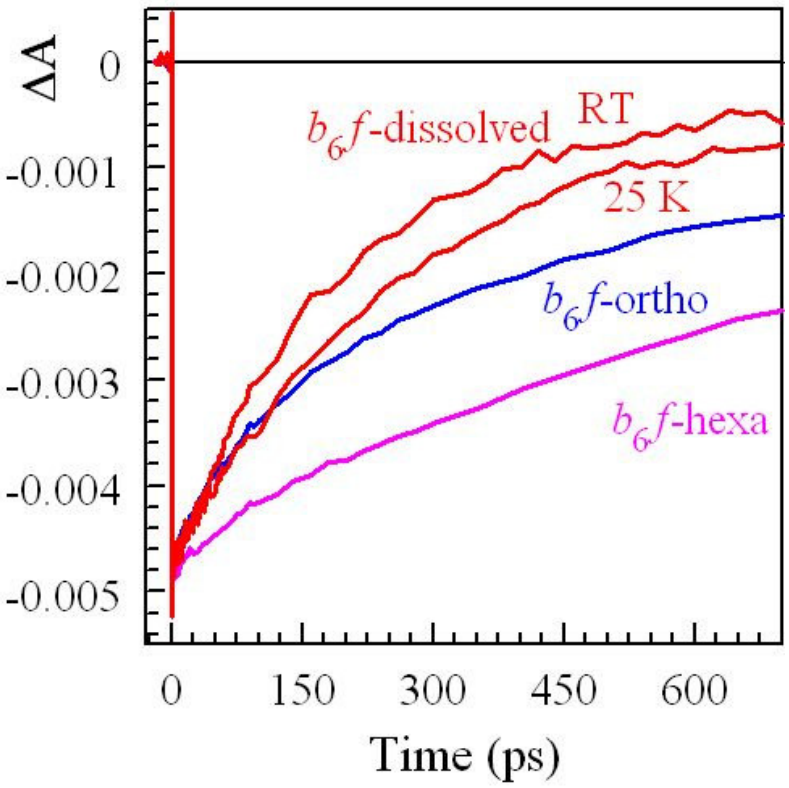
ΔA
0
-0.001
-0.002
-0.003
-0.004
-0.005
0
150
300
450
600
Time (ps)
b_6f-dissolved
RT
25 K
b_6f-ortho
b_6f-hexa

Figure 3

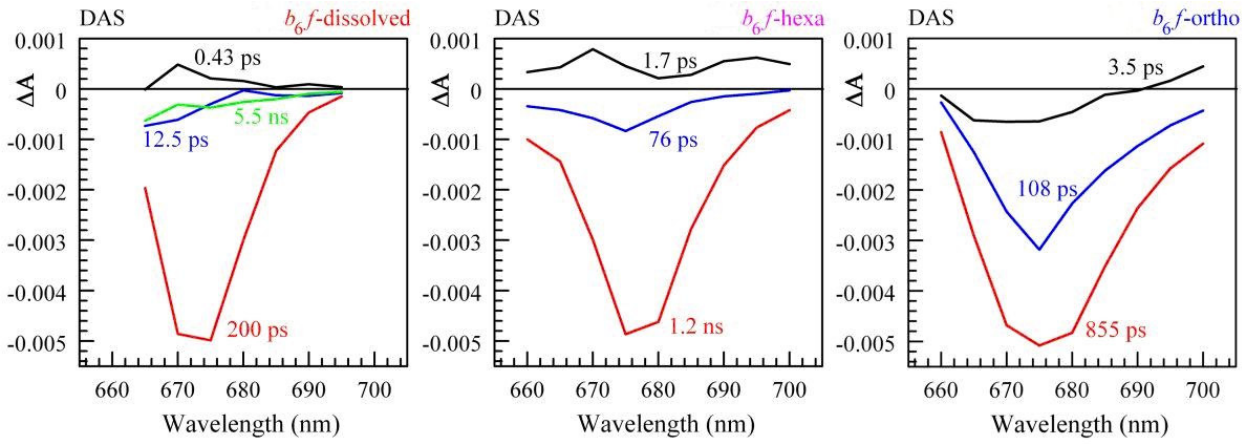
DAS
b_6f-dissolved
0.43 ps
5.5 ns
12.5 ps
200 ps
DAS
b_6f-hexa
1.7 ps
76 ps
1.2 ns
DAS
b_6f-ortho
3.5 ps
108 ps
855 ps
ΔA
0.001
0
-0.001
-0.002
-0.003
-0.004
-0.005
660
670
680
690
700
Wavelength (nm)

Figure 4

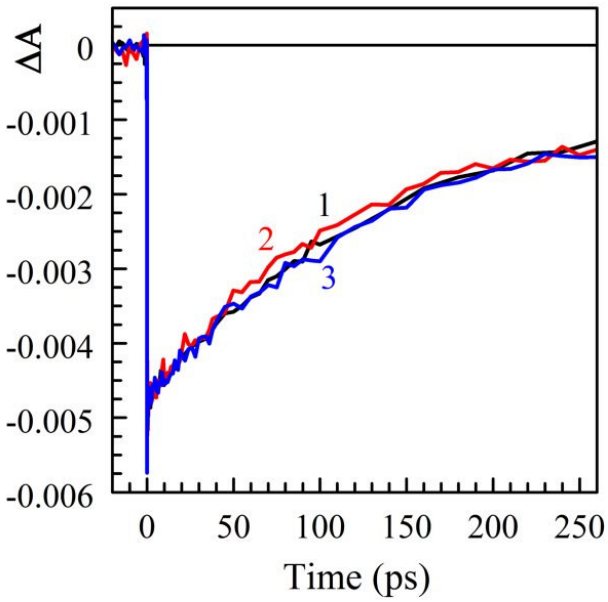
ΔA
0
-0.001
-0.002
-0.003
-0.004
-0.005
-0.006
0
50
100
150
200
250
Time (ps)
1
2
3

Figure 5